

# **A meta-analysis of open-path eddy covariance observations of apparent CO<sub>2</sub> flux in cold conditions in the FLUXNET network**

Liming Wang<sup>a,b,c,d</sup>, Xuhui Lee<sup>b,c</sup>, Wei Wang<sup>b,e</sup>, Xufeng Wang<sup>f</sup>, Zhongwang Wei<sup>b,c</sup>, Congsheng Fu<sup>b,c</sup>, Yunqiu Gao<sup>b,c</sup>, Ling Lu<sup>f</sup>, Weimin Song<sup>a,d</sup>, Peixi Su<sup>f</sup>, Guanghui Lin<sup>a,d</sup>

<sup>a</sup>Ministry of Education Key Laboratory for Earth System Modeling, Department of Earth System Science, Tsinghua University, Beijing 100084, China;

<sup>b</sup>Yale-NUIST Center on Atmospheric Environment, Nanjing University of Information Science and Technology, Nanjing 210044, China

<sup>c</sup>School of Forestry and Environmental Studies, Yale University, New Haven, Connecticut 06511, USA.

<sup>d</sup>Division of Ocean Science and Technology, Graduate School at Shenzhen, Tsinghua University, Shenzhen 518055, China

<sup>e</sup>Collaborative Innovation Center of Atmospheric Environment and Equipment Technology, Nanjing University of Information Science and Technology, Nanjing 210044, China

<sup>f</sup>Cold and Arid Regions Remote Sensing Observation System Experiment Station, Cold and Arid Regions Environmental and Engineering Research Institute, Chinese Academy of Sciences, Lanzhou 730000, China

## **Correspondence to:**

Xuhui Lee: [xuhui.lee@yale.edu](mailto:xuhui.lee@yale.edu); Guanghui Lin: [lingh@tsinghua.edu.cn](mailto:lingh@tsinghua.edu.cn)



## Abstract

Open-path eddy covariance systems are widely used for measuring the CO<sub>2</sub> flux between the land and the atmosphere. A common problem is that they often yield negative fluxes or physiologically unreasonable CO<sub>2</sub> uptake fluxes in the non-growing season under cold conditions. In this study, we performed a meta-analysis of the eddy flux data from 64 FLUXNET sites and analyzed the relationship between the observed CO<sub>2</sub> flux and the sensible heat flux. In theory, these two fluxes should be independent of each other in the cold conditions (air temperature lower than 0 °C) when photosynthesis is suppressed. However, our results show that a significant and negative linear relationship existed between these two fluxes at 37 of the sites. The mean linear slope value is  $-0.008 \pm 0.001 \mu\text{mol m}^{-2} \text{s}^{-1} \text{ per W m}^{-2}$  among the 64 sites analyzed. The slope value was not significantly different among the three gas analyzer models (LI-7500, LI-7500A, IRGASON/EC150) used at these sites, indicating that self-heating may not be the only reason for the apparent wintertime net CO<sub>2</sub> uptake. These results suggest a systematic bias towards larger carbon uptakes in the FLUXNET sites that deploy open-path EC systems.

**Keywords:** Eddy flux; Self-heating; Spectroscopic effects; Air temperature; Absolute humidity; CO<sub>2</sub> density

## 1. Introduction

The eddy-covariance (EC) technique is widely used for measuring exchanges of carbon dioxide between terrestrial ecosystems and the atmosphere. In the global EC network (FLUXNET), about half of the sites located north of 40° N deploy open-path CO<sub>2</sub>/H<sub>2</sub>O analyzers for flux measurements. Compared to closed-path analyzers, open-path analyzers need less power and less maintenance, and thus are better suited for remote locations. However, a physiologically unreasonable CO<sub>2</sub> uptake phenomenon has been reported frequently for cold seasons when no photosynthetic activities exist (Hirata et al. 2005; Welp et al. 2007; Lafleur and Humphreys 2008; Järvi et al. 2009; Wang et al. 2016) or for environments where CO<sub>2</sub> uptake is not expected (Liu et al. 2012; Ma et al. 2014; Ono et al. 2008; Wohlfahrt et al. 2008). Specifically, for desert ecosystems, Schlesinger (2017) argued that abiotic CO<sub>2</sub> uptake mechanisms like atmospheric pressure pumping, carbonate dissolution, and percolation of soil water through the vadose zone can not adequately explain the observation of EC systems. Following the micrometeorological sign convention, the uptake phenomenon is marked by a negative CO<sub>2</sub> flux or a flux directed towards the surface. According to Amiro et al. (2006) and other research groups (e.g., Burba et al. 2008; Helbig et al. 2016), the problem is not caused by software or hardware malfunction. Accurate CO<sub>2</sub> flux measurement is important for evaluating the global CO<sub>2</sub> cycle, terrestrial ecosystem responses to climate change, and modelling studies. Long-term integrated carbon flux will suffer a systematic bias if corrections are not made to the apparent flux in the cold season (Burba et al. 2008) or even in the whole year (Helbig et al. 2016).

Several explanations for the apparent negative flux are found in the published literature.

Self-heating of an open-path instrument is considered as a major reason for the negative flux (Burba et al. 2005; Burba et al. 2008; Grelle and Burba 2007). Because of heat release by the instrument's electronics and solar radiation heating of the instrument supporting frame, the air in the sensing volume of the analyzer may be warmer than the undisturbed air. Density corrections using the sensible heat flux measured outside the sensing volume cannot fully remove the effects of temperature fluctuations on CO<sub>2</sub> density fluctuations in the sensing volume. It is estimated that in mild temperatures (about 12 °C), the sensible heat flux in ambient air is 14% lower than the flux involving the actual temperature fluctuations in the sensing volume, and this rate of underestimation should increase as temperature decreases (Burba et al. 2008). The apparent cold-season CO<sub>2</sub> uptake was first observed with an older analyzer model manufactured by Li-Cor Inc (model LI-7500, Li-Cor Inc, Lincoln, Nebraska). To reduce the self-heating effect, the manufacturer has introduced an improved model (LI-7500A) with reduced power consumption during cold periods (Burba 2013). However, using a LI-7500A analyzer in their open-path EC system, Wang et al. (2016) found that there is still an apparent CO<sub>2</sub> uptake in a desert ecosystem in low temperatures (mean air temperature -6.7 °C), implying that other sources of wintertime bias exists for LI-7500A, if this gas analyzer indeed avoids the self-heating effect according to its producer.

Another explanation for the uptake phenomenon is related to the spectroscopic effects. Spectroscopic effects result from changes in the shape and the strength of CO<sub>2</sub> absorption lines; these changes are caused by changes in temperature, water vapor and pressure. If these effects are not properly dealt with, the fluctuations can be interpreted as changes in the

concentration of the gas (Welles & McDermitt 2005; Detto et al. 2011; McDermitt et al. 2011). These effects fall into two types: insufficient compensation due to high-frequency temperature fluctuations (Helbig et al. 2016) and spectroscopic cross-sensitivity (Kondo et al. 2014). In a class of analyzers (models IRGASON and EC150, Campbell Sci Inc., Logan, Utah) that use EC operating software released before September, 2016, the CO<sub>2</sub> density is determined by a scaling law (Jamieson et al. 1963) with temperature measured by a slow-responding thermometer mounted outside the analyzer's sensing volume. In an experiment that compared an open-path EC system using an IRGASON analyzer and a closed-path EC system, Bogoev et al. (2014) found that the CO<sub>2</sub> flux measured with the open-path EC is biased low and the low bias scales linearly with sensible heat flux. These authors and Helbig et al. (2015 & 2016) showed that this spectroscopic effect can be corrected by using fast-response air temperature measurements to perform the absorption line calculation. After this correction, the linear relationship between the corrected CO<sub>2</sub> flux and the heat fluxes almost disappears. Unlike the self-heating effect, which is believed to be limited only to cold seasons, this spectroscopic error exists in all seasons. At low temperatures when the true CO<sub>2</sub> flux is very small, the flux measured with an IRGASON may appear negative (Wang et al. 2016). It is not known to what extent spectroscopic effects affect the CO<sub>2</sub> flux measured with other open-path analyzers.

Spectroscopic cross-sensitivity can arise from a pressure broadening effect and from absorption line interference between CO<sub>2</sub> and H<sub>2</sub>O. Generally, the absorption interference is much smaller than the pressure broadening effect (Kondo et al. 2014). These effects are

corrected by using measurements of air pressure and H<sub>2</sub>O mole fraction and manufacturer-determined correction coefficients. Kondo et al. (2014) found that for a LI-7200 gas analyzer with the same design as the LI-7500, the manufactured correction coefficient for spectroscopic cross-sensitivities results in an overestimation of CO<sub>2</sub> mixing ratio by about 0.9% at a H<sub>2</sub>O mole fraction of 30.6 mmol mol<sup>-1</sup>. Different from the effect associated with high-frequency temperature fluctuations, this spectroscopic cross-sensitivity biases the CO<sub>2</sub> flux towards more positive values, and the biases increase with the H<sub>2</sub>O mole fraction. Because this influence is much smaller than the other bias sources, in the following we will not examine this problem.

Finally, a negative CO<sub>2</sub> flux in the cold season can result from errors propagated through the density correction procedure. The WPL density correction requires that the CO<sub>2</sub> density ( $\rho_c$ ) be measured precisely. But in field conditions, biases in  $\rho_c$  can be caused by thermal expansion and contraction of the analyzer's frame on which the transducers are mounted, by dirt contamination on the transducers, and by aging of the optical components (Fratini et al. 2014). An underestimation of  $\rho_c$  will cause CO<sub>2</sub> flux to be too negative (Serrano-Ortiz et al. 2008). The bias in the CO<sub>2</sub> flux scales linearly with the sensible heat flux if the CO<sub>2</sub> density is underestimated by a constant amount.

In this study, we perform a meta-analysis of the eddy flux data from 64 sites located in North America, Europe, Asian and Australia, and analyze the relationship between the apparent CO<sub>2</sub> flux and the sensible heat flux in cold conditions. We aim to: 1) compare the negative bias

problem among different open-path gas analyzers, and 2) investigate the bias errors in relation to climatic conditions (temperature, humidity) and to biases in the CO<sub>2</sub> concentration.

## 2. Data and Methods

### 2.1 Theoretical Consideration

#### Self-heating

The CO<sub>2</sub> flux bias error arising from self-heating can be understood by examining the WPL algorithm (Webb et al. 1980),

$$(1)$$

where  $F_{c,a}$  is the CO<sub>2</sub> flux after density correction ( $\text{kg m}^{-2} \text{s}^{-1}$ ),  $w$  is the vertical wind velocity ( $\text{m s}^{-1}$ ),  $\rho_c$  and  $\rho_a$  are density of CO<sub>2</sub> ( $\text{kg m}^{-3}$ ) and dry air ( $\text{kg m}^{-3}$ ),  $T$  is the air temperature (K),  $M$  is the molecular mass ( $\text{g mol}^{-1}$ ),  $C_p$  is the specific heat of air ( $\text{J kg}^{-1} \text{K}^{-1}$ ),  $H$  is the sensible heat flux ( $\text{W m}^{-2}$ ) measured in ambient air outside the analyzer's sensing volume,  $E_0$  is the H<sub>2</sub>O flux ( $\text{kg m}^{-2} \text{s}^{-1}$ ), and subscripts a, v, and c represent dry air, water vapor, and CO<sub>2</sub>, respectively. Let  $H_{\text{real}}$  be the real sensible heat inside the open path. To obtain the correct CO<sub>2</sub> flux,  $F_c$ , Equation (1) should be modified to, (2)

A comparison of Equations (1) and (2) yields

$$(3)$$

According to Burba et al. (2008), the sensible heat flux measured in the ambient air ( $H$ ) is highly correlated with the sensible heat flux inside the open path measured with a fine-wire platinum resistor ( $H_{\text{real}}$ ). Their linear relationship is,



(4)

where  $\alpha = 0.86$  and  $\beta = 2.67 \text{ W m}^{-2}$ .

The Equation (3) can be rewritten as

(5)

where

(6)

(7)

For  $\alpha = 0.86$ ,  $\beta = 2.67$ , the slope parameter  $b$  in Equation (6) is approximately  $-0.008 \text{ } \mu\text{mol m}^{-2} \text{ s}^{-1}$  per  $\text{W m}^{-2}$  after unit conversion (from  $\text{kg m}^{-2} \text{ s}^{-1}$  per  $\text{W m}^{-2}$  to  $\mu\text{mol m}^{-2} \text{ s}^{-1}$  per  $\text{W m}^{-2}$ , divided by  $\text{CO}_2$  molar mass), and the parameter  $a$  is approximately  $-0.16 \text{ } \mu\text{mol m}^{-2} \text{ s}^{-1}$ .

Equation (5) predicts that negative  $F_{\text{c,a}}$  is more likely to occur at times of high sensible heat flux. An implicit assumption is that sensor self-heating is dominated by solar radiation rather than heating caused by the sensor electronics. We also hypothesize that  $b$  is more negative for colder sites since the self-heating effect is expected to be more severe.

### **Insufficient compensation for spectroscopic effects**

Spectroscopic effects affect every instrument that measures absorption or IRGASON/EC150 gas analyzers, which are subject to insufficient compensation for spectroscopic effects due to

high-frequency temperature fluctuations, the observed flux  $F_{c,a}$  and the true flux  $F_c$  also follows the linear relationship with the ambient sensible heat flux (Bogoev et al. 2014; Helbig et al. 2015; Helbig et al. 2016), as given by Equation (5). A theoretical slope value can be described as (Wang et al. 2016),

$$(8)$$

Under typical atmospheric conditions, the theoretical value for  $b$  is about  $-0.025 \mu\text{mol m}^{-2} \text{s}^{-1} \text{ per W m}^{-2}$ . A comparison of an IRGASON open-path EC versus a closed-path EC reveals that the actual slope is about half of the theoretical value, at  $-0.014 \mu\text{mol m}^{-2} \text{s}^{-1} \text{ per W m}^{-2}$  (Bogoev et al. 2014). Subsequent experiments by Helbig et al. (2015 & 2016) in boreal forest, grassland and cropland sites showed that the slope value ranges from  $-0.014$  to  $-0.020 \mu\text{mol m}^{-2} \text{s}^{-1} \text{ per W m}^{-2}$  and that the intercept value ( $a$ ) ranges from  $-0.300$  to  $0.080 \mu\text{mol m}^{-2} \text{s}^{-1}$ .

#### **Biases in CO<sub>2</sub> density**

Bias errors in the CO<sub>2</sub> density  $\rho_c$  can also be examined in the framework of the WPL theory. Let  $\bar{\rho}_c$  be the true mean CO<sub>2</sub> density, and  $b$  be the measurement bias. The measured flux  $F_{c,a}$  after the WPL correction is,

$$(9)$$

with the slope parameter given by

$$(10)$$

In Equation (9),  $LE$  is the latent heat flux and  $\lambda$  is the latent heat of vaporization. The

magnitude of  $LE$  is comparable with  $H$ , and the term before  $LE$  is equal to  $0.004 \text{ (}\mu\text{mol m}^{-2} \text{ s}^{-1} \text{ per W m}^{-2}\text{)}$ , which is one order of magnitude smaller than  $0.05 \text{ (}\mu\text{mol m}^{-2} \text{ s}^{-1} \text{ per W m}^{-2}\text{)}$  in Equation (10). Thus, we ignored this term to simplify the analysis.

In the situation where  $\beta$  is underestimated by 10% (; Serrano-Ortiz et al. 2008), the slope  $b$  is approximately  $-0.005 \mu\text{mol m}^{-2} \text{ s}^{-1} \text{ per W m}^{-2}$ .

## 2.2 Data sources and data processing

The eddy flux data analyzed in the present study were obtained from the AmeriFlux, the FLUXNET, the ChinaFlux, and the Chinese Heihe databases. The majority of the sites are located north of  $40^\circ \text{ N}$  (Figure 1; Tables S1 & S2). These sites have continuous eddy flux records for at least 5 days when the air temperature is below the freezing point in the winter. There are a total of 64 sites, including 57 sites using LI-7500, 6 sites using LI-7500A and one site using IRGASON. The eddy flux data at 28 sites were obtained from the FLUXNET. These data have been gap filled and through a Ustar-threshold filtering following the FLUXNET data processing pipeline. The other eddy flux data, obtained from the AmeriFlux (20 sites), the ChinaFlux (7 sites) and the Heihe databases (9 sites), were not gap-filled and without the Ustar-threshold filtering.

When the air temperature is below  $0^\circ \text{ C}$  in the winter (January, February and December in the Northern Hemisphere; June, July and August in Australia), the true carbon flux  $F_c$  should be slightly positive due to ecosystem respiration, but should be very small and independent of

the sensible heat flux  $H$  due to suppression of photosynthesis. We assume that any correlation between the measured flux  $F_{c,a}$  and  $H$  is evidence of measurement errors. For each site, we only used winter data when the half-hourly or hourly air temperature was below 0 °C, and applied the ordinary linear regression to the observed CO<sub>2</sub> flux and sensible heat flux, using the sensible heat flux as the independent variable. The regression yields the slope parameter  $b$  and intercept parameter  $a$ . We then tried to discern patterns of the slope parameter among the 64 sites. Half hourly or hourly data influenced by precipitation were excluded from the regression analysis. We also restricted the sensible heat flux to the range of -100 to 400 W m<sup>-2</sup> and the latent heat flux to the range of -200 to 700 W m<sup>-2</sup> to avoid extreme values due to unknown measurement errors. The CO<sub>2</sub> flux was limited in -10 to 10 μmol m<sup>-2</sup> s<sup>-1</sup>. Prior to the regression, the half-hourly or hourly data were averaged by every 20 W m<sup>-2</sup> bin of sensible heat flux to reduce the effect of random measurement errors on the parameter estimation.

We used the CO<sub>2</sub> mole fraction data from CarbonTracker (version CT2016, global 3°×2° grid, level 1) to calculate the bias in the CO<sub>2</sub> density  $\rho_c$  measured by the EC open-path analyzers. CarbonTracker is a data inversion system aiming to calculate global CO<sub>2</sub> fluxes from high precision atmospheric CO<sub>2</sub> measurements. Peters et al. (2007) compared the optimized three dimensional CO<sub>2</sub> mole fraction fields produced by CarbonTracker with 13,000 independent CO<sub>2</sub> flask samples taken in the free troposphere, and found that the mean and standard deviation of the residuals are 0.07 ppm and 1.91 ppm, respectively.

To determine the bias error in the CO<sub>2</sub> density, we first selected a CarbonTracker grid cell that is closest to the measurement site. We then chose the CarbonTracker surface CO<sub>2</sub> mole fraction for those days when the actual flux data were used for our analysis. The mean CarbonTracker CO<sub>2</sub> mole fraction of those measurement days is regarded as the true CO<sub>2</sub> mole fraction. Finally, the bias ratio in CO<sub>2</sub> mass density ( $\rho$ ) is represented by the bias ratio of the CO<sub>2</sub> mole fraction (CO<sub>2</sub> concentration is given by mole fraction in FLUXNET) since the pressure and temperature effects are canceled out.

### 3. Results and Discussion

#### 3.1 Relationship between observed $F_{c,a}$ and $H$

A significant ( $p < 0.05$ ) and negative correlation exists between the observed  $F_{c,a}$  and  $H$  at 37 of the 64 sites, and only 4 sites have significant and positive correlation. The mean coefficient of determination ( $R^2$ ) is 0.63 for all the sites. The regression statistics are shown in Supplementary Table S1 and the scatter plots for individual sites are given in Figure S1. Among the sites analyzed, 45 sites have  $R^2$  value larger than 0.5.

We also analyzed the relationship between the apparent CO<sub>2</sub> flux and the incoming solar radiation. The mean  $R^2$  is 0.48 for the 39 sites that have the radiation data. Among these sites, 17 sites have  $R^2$  values larger than 0.5. The results show that  $H$  is a better independent variable than solar radiation to do this analysis.

We analyzed the relationship of CO<sub>2</sub> flux and sensible heat measured by a closed-path

analyzer at site AT-Neu in the cold season, and we found that this relationship is insignificant ( $p = 0.13$ ,  $R^2 = 0.26$ ). The result supports our hypothesis that the true carbon flux  $F_c$  should be independent of the sensible heat flux  $H$ . On the other hand, the relationship for the open-path measurement at this site is significant ( $p = 0.017$ ,  $R^2 = 0.71$ ).

Figure 2 shows two examples. At a shrub land ecosystem in the Kubuqi desert in China (site ID: CN-Kub\_s; analyzer type: LI-7500; Figure 2a), the linear relationship can be described as

$$(11)$$

where  $F_{c,a}$  is the observed carbon flux ( $\mu\text{mol m}^{-2} \text{s}^{-1}$ ),  $H$  is sensible heat ( $\text{W m}^{-2}$ ). The error bounds on the regression parameters are  $\pm 1$  standard error. In this case, the negative correlation between  $F_{c,a}$  and  $H$  is very strong, with an  $R^2$  value of 0.99 and the p-value smaller than 0.0001.

Not all the sites have such a nearly perfect linear relationship between  $F_{c,a}$  and  $H$  as shown in Figure 2a. For example, the relationship is much weaker for the Brook cropland site in the U. S. (site ID: US-Br3; analyzer type: LI-7500; Figure 2b). The linear equation for this site is given as

$$(12)$$

with  $R^2 = 0.38$  and a p-value of 0.79. US-Br3 is one of the 15 sites that show a large scatter around  $H = 0$ . Nine of them belong to the cold climate zone and the other 6 sites belong to the mild temperature zone. None is found in the arid zone and the polar region. Perhaps the scatter was caused by moisture interferences (dew formation or rain). Significant negative

correlation exists between the site-mean CO<sub>2</sub> flux and the site mean sensible heat flux (Supplementary Figure S2).

The regression slope  $b$  ranges from  $-0.051$  to  $0.013 \mu\text{mol m}^{-2} \text{s}^{-1} \text{ per W m}^{-2}$  with an average value of  $-0.008 \mu\text{mol m}^{-2} \text{s}^{-1} \text{ per W m}^{-2}$  among the 64 sites analyzed. For the sites listed in Table S1, 84% have a negative slope and 16% have a positive slope. The frequency histogram shows that 38% of them range from  $-0.015 \mu\text{mol m}^{-2} \text{s}^{-1} \text{ per W m}^{-2}$  to  $-0.007 \mu\text{mol m}^{-2} \text{s}^{-1} \text{ per W m}^{-2}$ , and 67% of them range from  $-0.015 \mu\text{mol m}^{-2} \text{s}^{-1} \text{ per W m}^{-2}$  to  $0.00 \mu\text{mol m}^{-2} \text{s}^{-1} \text{ per W m}^{-2}$  (Figure 3). The mean slope of the 28 FLUXNET sites, whose data have been gap-filled and through a Ustar-threshold filtering, is  $-0.009 \pm 0.0004 \mu\text{mol m}^{-2} \text{s}^{-1} \text{ per W m}^{-2}$ , and is not significantly different from the mean slope of other sites ( $-0.007 \pm 0.0003 \mu\text{mol m}^{-2} \text{s}^{-1} \text{ per W m}^{-2}$ ;  $p = 0.45$ ). Here and hereafter, the variation range on  $b$  is expressed as  $\pm$  one standard error. The difference between vegetation types considered is not statistically significant ( $p = 0.70$ , Figure S3).

We compared the slope of the sites that deployed the CSAT3 anemometer to measure the turbulent velocity and those that deployed the Gill anemometer. The mean slope  $b$  is  $-0.008 \pm 0.001 \mu\text{mol m}^{-2} \text{s}^{-1} \text{ per W m}^{-2}$  for the CSAT3 sites (number of sites  $n = 46$ ) and  $-0.008 \pm 0.002 \mu\text{mol m}^{-2} \text{s}^{-1} \text{ per W m}^{-2}$  for the Gill sites ( $n = 17$ ). The difference between these two groups is statistically insignificant ( $p = 0.92$ ). For the site (Site ID: JP-SMF) deployed the DAT-540 anemometer (Kaijo, Japan), the slope  $b$  is  $-0.010 \mu\text{mol m}^{-2} \text{s}^{-1} \text{ per W m}^{-2}$ . It should be mentioned that biases in  $H$  can be also caused by sonic anemometer measurement errors,

such as the angle of attack errors with Gill anemometers (Nakai et al. 2006; Nakai and Shimoyama 2012) and transducer shadowing effects on CSAT3 (Horst et al. 2015) and IRGASON (Horst et al. 2016).

The comparison among the three models of gas analyzer is given in Figure 4. The mean slope value for the sites that deployed LI-7500 is  $-0.007 \pm 0.001 \mu\text{mol m}^{-2} \text{s}^{-1}$  per  $\text{W m}^{-2}$  ( $n = 54$ ), excluding three sites (site ID: US-ICH, US-ICs and FR-Fon, with slope values of 0.011,  $-0.008$  and  $-0.009$ , respectively), which are suspected to have archived the flux data after self-heating correction (Euskirchen et al. 2012; Delpierre et al., 2015). As for the LI-7500A sites, the average slope value is  $-0.012 \pm 0.002 \mu\text{mol m}^{-2} \text{s}^{-1}$  per  $\text{W m}^{-2}$  ( $n = 6$ ). The problem did not go away with LI-7500A despite hardware improvement over the older version LI-7500. Besides the result of the Tarim site (site ID: CN-Tarim2; Wang et al., 2016), we also acquired the slope values published for three other sites using IRGASON analyzers and one site using an EC150 analyzer (Helbig et al. 2016). In that paper, the slopes were calculated for  $F_c$  and the kinematic temperature flux, and we used air density and specific heat capacities under typical atmospheric conditions to convert these values to slope values for the  $F_c$  and  $H$ . The mean slope is  $-0.013 \pm 0.001 \mu\text{mol m}^{-2} \text{s}^{-1}$  per  $\text{W m}^{-2}$  for these sites ( $n = 5$ ). The mean (and standard error)  $R^2$  of the LI-7500, the LI-7500A and the IRGASON/EC150 site group is 0.61 ( $\pm 0.04$ ), 0.76 ( $\pm 0.06$ ) and 0.77 ( $\pm 0.10$ ) respectively (Figure 4). The differences in the regression slope or  $R^2$  among the three analyzer types are not statistically significant ( $p > 0.30$ ).



The mean slope value and its standard error are compared among different climate zones according to Köppen climate classification (Figure 5). The sites in the temperate zone have the most negative mean slope value ( $-0.012 \pm 0.003 \mu\text{mol m}^{-2} \text{s}^{-1} \text{ per W m}^{-2}$ ,  $n = 17$ ), those in the polar zone have the least negative mean value ( $-0.001 \pm 0.003 \mu\text{mol m}^{-2} \text{s}^{-1} \text{ per W m}^{-2}$ ,  $n = 6$ ), and sites in the arid zone ( $-0.009 \pm 0.002 \mu\text{mol m}^{-2} \text{s}^{-1} \text{ per W m}^{-2}$ ,  $n = 16$ ) and the cold zone ( $-0.006 \pm 0.002 \mu\text{mol m}^{-2} \text{s}^{-1} \text{ per W m}^{-2}$ ,  $n = 25$ ) fall between these two mean values. The differences in the slope value may potentially reflect  $\text{CO}_2$  flux measurement biases in different background air temperature, humidity and  $\text{CO}_2$  density in different climate zones.

### 3.2 Self-heating effect

According to our analysis in section 2.1, if self-heating is the main reason to explain the linear relationship between the apparent  $\text{CO}_2$  flux and  $H$  and if the linear relationship between  $H$  and  $H_{\text{real}}$  reported by Burba et al. (2008) holds, the slope  $b$  should be  $-0.008 \mu\text{mol m}^{-2} \text{s}^{-1} \text{ per W m}^{-2}$ . This expected value is very close to the mean value of  $-0.007 \pm 0.001 \mu\text{mol m}^{-2} \text{s}^{-1} \text{ per W m}^{-2}$  of the 54 sites that deployed the LI-7500 analyzer (Figure 4).

Burba et al. (2008) also postulates that self-heating should be more severe in colder conditions, meaning that the slope should be more negative as the site temperature decreases, so a positive correlation is expected between the slope parameter  $b$  and the site mean temperature. We plot the regression slope with the site mean air temperature (Figure 6a) to test this postulation, and find that the Pearson's correlation coefficient between the slope and

temperature is slightly negative ( $-0.2$ ) and the correlation is not significant ( $p = 0.13$ ). The correlation with site mean absolute humidity is not statistically significant either (Figure 6b). This single-variable correlation can be confounded by bias errors in the  $\text{CO}_2$  density. Thus, we first calculated  $b$  caused by  $\delta\rho_c$  using Equation (10) and then subtracted this value from the regression slope for each site. The resulting slope residual still does not show a positive linear relationship with air temperature (Figure S4). In other words, our meta-analysis failed to uncover a climatic pattern regarding the self-heating effect.

### 3.3 Comparison among analyzer types

The slope among the sites that deployed either the IRGASON or the EC150 analyzer is all negative and varies in a narrow range from  $-0.019$  to  $-0.011 \mu\text{mol m}^{-2} \text{s}^{-1}$  per  $\text{W m}^{-2}$ , giving a mean value of  $-0.013 \mu\text{mol m}^{-2} \text{s}^{-1}$  per  $\text{W m}^{-2}$  (Figure 4). This mean value is 86 % greater in magnitude than the mean value obtained for the LI-7500 analyzers, but the difference is not statistically significant ( $p = 0.14$ ). Because the IRGASON is an integrated system whose measurements of the  $\text{CO}_2$  concentration and the temperature are made in the same sensing volume, any sensor self-heating would be automatically detected and be removed by the WPL correction procedure. Instead, the correlation between the  $\text{CO}_2$  flux bias and the sensible heat flux is a result of the spectroscopic effect. The same spectroscopic effect also exists for the EC150 gas analyzer (Helbig et al. 2016).

As for LI-7500, Welles & McDermitt (2005), Fratini et al. (2014) and Helbig et al. (2016) believed that the air temperature only marginally affects the broadband measurements, so the

spectroscopic effect can be ignored. Our results show that, for LI-7500, the slope varies in a wider range from  $-0.051$  to  $0.013 \mu\text{mol m}^{-2} \text{s}^{-1} \text{ per W m}^{-2}$ , with a mean value of  $-0.007 \mu\text{mol m}^{-2} \text{s}^{-1} \text{ per W m}^{-2}$ . The average slope value is less negative than the result of IRGASON/EC150. Thus, we infer that the spectroscopic effect, if there is any, should be weaker for LI-7500 than for IRGASON/EC150.

The slopes for the 6 sites that deployed the LI-7500A gas analyzer are all negative, ranging from  $-0.017$  to  $-0.003 \mu\text{mol m}^{-2} \text{s}^{-1} \text{ per W m}^{-2}$ , with a mean value of  $-0.012 \mu\text{mol m}^{-2} \text{s}^{-1} \text{ per W m}^{-2}$ . This mean value is 71 % greater in magnitude than the mean value for LI-7500, but the difference is also not significant ( $p = 0.16$ ). According to the manufacturer (Burba 2013), LI-7500A has been improved over LI-7500 to reduce the self-heating effect. Our result suggests that the apparent uptake problem still exists for this type of analyzers, at least for the 6 sites we have analyzed (Figure S1). This result suggests that surface heating may not be the only reason for the apparent wintertime net  $\text{CO}_2$  uptake.

Using an open-path EC system consisting of a LI-7500A analyzer and a Gill anemometer, Wang et al. (2016) observed a midday uptake flux of  $-1.6 \mu\text{mol m}^{-2} \text{s}^{-1}$  at a desert ecosystem in the winter (mean air temperature  $-6.7^\circ\text{C}$ ). They estimated that if self-heating were the cause, this negative flux would require an amount of self-heat equivalent to  $31 \text{ W m}^{-2}$ . However, the mean difference between the sensible heat fluxes derived from the two sonic anemometers is only about  $0.4 \text{ W m}^{-2}$ . In their study, the apparent uptake flux measured with the LI-7500A analyzer is nearly the same as that measured with an IRGASON EC system. It

is interesting that the mean slope for LI-7500A is nearly the same as that for IRGASON/EC150 (Figure 4). Similar to IRGASON/EC150, the open-path methane analyzer described by Burba et al. (2010) may need correction to account the spectroscopic effect due to temperature fluctuations. Our current understanding of the LI-7500A analyzers is inadequate to draw a firm conclusion as to whether they have the same type of errors.

### 3.4 Bias in gas concentration measurements

As explained in Section 2.1, errors in the CO<sub>2</sub> concentration measurements affect the CO<sub>2</sub> flux measurement. Underestimation of  $\rho_c$  will result in a negative slope value in the regression of the measured CO<sub>2</sub> flux versus the sensible heat flux. In the current study, the bias in the CO<sub>2</sub> concentration was calculated as the measured value minus the CarbonTracker result. To examine how well the surface CO<sub>2</sub> concentration produced by CarbonTracker represents the true CO<sub>2</sub> concentration, we compared the monthly CarbonTracker concentration in the winter (January, February and December) with the measurement made with closed-path analyzers at Harvard Forest in the U. S. and at Old Aspen in Canada (site IDs: US-Ha1 and CA-Oas). At these sites, the closed-path analyzers (model LI-6262) were calibrated periodically against CO<sub>2</sub> standard gases traceable to the World Meteorological Organization (WMO) standards (Bakwin et al. 2004; Krishnan et al. 2006), so the concentration measurements are in high quality. In a scatter plot, the results lie near the 1:1 line, with R<sup>2</sup> equal to 0.77 and 0.89 for Harvard Forest and Old Aspen, respectively (Figure S5). On average, the residual (CarbonTracker minus observation) is  $-1.9 \pm 5.2$  ppm (mean  $\pm$  1 SD) at Harvard Forest and  $-0.1 \pm 2.6$  ppm (mean  $\pm$  1 SD) at Old Aspen. This comparison

supports the use of CarbonTracker CO<sub>2</sub> concentration as a benchmark to evaluate bias errors in  $\rho_c$  measured with open-path analyzers.

Among the 51 sites having CO<sub>2</sub> concentration measurement records, the bias ratio ranges from –18 % to 6 %, with a mean value of –5 %. Of these sites, 45 sites show a negative bias. The tendency to observe low biases with open-path analyzers in the cold season may be related to thermal contraction of the analyzer’s optical path (Fratini et al. 2014) or lack of frequent calibration. At these northern sites, it is common to perform instrument calibration in the warm season when the sites are more accessible than in the cold season.

According to Equation (10), under typical atmosphere conditions, the regression slope  $b$  should be approximately equal to. At the averaged CO<sub>2</sub> concentration bias ratio of –0.05, the corresponding slope  $b$  is  $-0.0025 \mu\text{mol m}^{-2} \text{s}^{-1} \text{ per W m}^{-2}$ , or about 30% of the mean value of  $-0.008 \pm 0.001 \mu\text{mol m}^{-2} \text{s}^{-1} \text{ per W m}^{-2}$  of the sites we analyzed.

The Pearson’s correlation coefficient between the slope parameter  $b$  derived from measurements and is 0.04. There is no significant linear relationship between  $b$  and the bias in the CO<sub>2</sub> density (Figure 7,  $p = 0.99$ ). The three outliers in Figure 7 are US-Wi5 ( $b = -0.051 \mu\text{mol m}^{-2} \text{s}^{-1} \text{ per W m}^{-2}$ ), DE-RuS ( $b = -0.037 \mu\text{mol m}^{-2} \text{s}^{-1} \text{ per W m}^{-2}$ ) and AT-Neu ( $b = -0.030 \mu\text{mol m}^{-2} \text{s}^{-1} \text{ per W m}^{-2}$ ).

### 3.5 Correcting wintertime CO<sub>2</sub> flux

Our analysis suggests that a systematic bias exists at many open-path EC sites in the FLUXNET network. A natural question is how to best correct the bias error. According to Equations (5) and (9), the true flux  $F_c$  is related to the measured flux  $F_{c,a}$  as

$$(13)$$

The mean value of  $a$  among the 64 sites is  $0.02 (\pm 0.10) \mu\text{mol m}^{-2} \text{s}^{-1}$ , which is higher than the value derived from self-heating theory (Section 2.1). In Bogoev et al. (2015), this interception term is  $0.067 \mu\text{mol m}^{-2} \text{s}^{-1}$  for an IRGASON analyzer. We consider this term as a bias source which is not scaled with  $H$  and site specific.

Figure 8 shows the diurnal composite of the flux for a shrubland site in Northern China (site ID: CN-Kub\_s) in December 2008 before and after correction using Equation (13) (regression parameter values  $b = -0.014 \mu\text{mol m}^{-2} \text{s}^{-1}$  per  $\text{W m}^{-2}$  and  $a = -0.28 \mu\text{mol m}^{-2} \text{s}^{-1}$ ). The mean air temperature during this month was  $-9.2^\circ\text{C}$ . The analyzer model was LI-7500. The original flux  $F_{c,a}$  is negative in the daytime, with the most negative value ( $-2 \mu\text{mol m}^{-2} \text{s}^{-1}$ ) occurring at noon when the sensible heat reaches the maximum value. The 24-hour mean value is  $-0.34 \mu\text{mol m}^{-2} \text{s}^{-1}$ . After the correction, the flux  $F_c$  appears much more reasonable: it varies in a very narrow range between  $-0.25 \mu\text{mol m}^{-2} \text{s}^{-1}$  and  $0.37 \mu\text{mol m}^{-2} \text{s}^{-1}$  in the daytime, and the 24-hour mean value is slightly positive ( $0.11 \mu\text{mol m}^{-2} \text{s}^{-1}$ ).

The correction procedure has a large impact on the cumulative carbon flux at this site. Without the correction, the annual net ecosystem productivity (NEP) is  $163 \text{ g C m}^{-2}$  in 2008 (Figure 9). Here, a positive NEP indicates that the ecosystem is a sink for atmospheric  $\text{CO}_2$ ,

and vice versa. If the correction is applied to the three winter months (December, January, February), the annual NEP will change to  $107 \text{ g C m}^{-2}$ . If the correction equation is applied to five months (November to March), the annual NEP will be  $62 \text{ g C m}^{-2}$  (Figure 9). If the correction is extended to the whole year, the annual NEP will be negative ( $-172 \text{ g C m}^{-2}$ ), implying that the site is a carbon source. A similar sensitivity is documented by Amiro et al. (2010), who showed that implementing the self-heating correction over varying time lengths results in contrasting annual NEP values at a burned boreal forest site.

At site AT-Neu (a grass land ecosystem in Austria), the annual NEP determined with an open-path gas analyzer (LI-7500) is  $-72 \text{ g C m}^{-2}$  in year 2003, while the result of a closed-path gas analyzer is  $-119 \text{ g C m}^{-2}$ . If the correction is applied to the three winter months (December, January, February;  $b = -0.03 \text{ } \mu\text{mol m}^{-2} \text{ s}^{-1} \text{ per W m}^{-2}$  and  $a = -0.39 \text{ } \mu\text{mol m}^{-2} \text{ s}^{-1}$ ), the annual NEP will change to  $-84 \text{ g C m}^{-2}$ . When the correction is extended to the whole year, the annual NEP will be  $-188 \text{ g C m}^{-2}$  (Figure 10). The result shows that some biases with the open-path flux may still exist in the warm season, but the regression parameters may be different from the values found for the cold season.

Our bias detection method assumes that the true  $\text{CO}_2$  flux is independent of the sensible heat flux. Obviously, this assumption does not hold in the warm season, because a high rate of photosynthesis tends to occur at times of a high sensible heat flux, so we cannot use the same method to detect flux bias errors in the warm season. Inter-comparisons of open-path and closed-path measurements are necessary in order to determine the relationship between the

flux bias errors and sensible heat flux in the warm season. In the case of IRGASON and EC150 analyzers, the correction equation (Equation (13); Bogoev et al. 2014; Wang et al. 2016; Helbig et al. 2016) established in the cold season should also be applicable to other months because the spectroscopic effect is the same all-year round.

#### 4. Conclusions

In this study, we analyzed the CO<sub>2</sub> and sensible heat flux data collected at 64 eddy flux sites in the cold season. A significant ( $p < 0.05$ ) and negative linear relationship between the observed CO<sub>2</sub> flux  $F_{c,a}$  and the sensible heat flux  $H$  was found for 37 of the sites, suggesting a systematic bias towards larger carbon uptakes in the FLUXNET network in the cold season. The mean regression slope was  $-0.007 \pm 0.001$ ,  $-0.012 \pm 0.002$  and  $-0.013 \pm 0.001$   $\mu\text{mol m}^{-2} \text{s}^{-1}$  per  $\text{W m}^{-2}$  for LI-7500, LI7500A and IRGASON/EC150 gas analyzers, respectively. The apparent uptake problem still exists for LI-7500A analyzers, even though LI-7500A has been improved over LI-7500 to reduce the self-heating problem. This result suggests that self-heating may not be the only reason for the apparent wintertime net CO<sub>2</sub> uptake observed at many eddy flux sites. The slope value did not show statistically significant linear relationships with local temperature and humidity.

On average, the CO<sub>2</sub> concentration measured at these sites (with open-path analyzers) in the cold season is biased low by 5 % in comparison to the CarbonTracker surface CO<sub>2</sub> concentration. The corresponding slope value is  $-0.0025$   $\mu\text{mol m}^{-2} \text{s}^{-1}$  per  $\text{W m}^{-2}$  and about 30% of the mean value of the 64 sites, but the slope value is only weakly correlated with the



site mean concentration bias.

We have documented post-field corrections to the CO<sub>2</sub> flux measured with the LI-7500 and LI-7500A analyzers in the cold season. At present, we do not have evidence supporting the application of these corrections for the whole year. Inter-comparisons of open-path and closed-path eddy covariance measurements are necessary to investigate whether similar bias errors exist in the warm season.

## **Acknowledgements**

This work is supported jointly by the Department of Earth System Science, Tsinghua University and the School of Forestry and Environmental Studies, Yale University. We are grateful for the financial support from National Basic Research Program of China (2013CB956601, 2013CB956604), The Publicly Funded Ocean Research Program, State Oceanic Administration of China (201305021) and China Scholarship Council. This work used eddy covariance data acquired by the FLUXNET community. We thank Professor Georg Wohlfahrt and the Chinese Heihe project scientists for their generous sharing of their eddy flux data. CarbonTracker CT2016 results are provided by NOAA ESRL, USA.

## References

- Amiro, B., 2010: Estimating annual carbon dioxide eddy fluxes using open-path analysers for cold forest sites. *Agricultural and Forest Meteorology*, **150**, 1366-1372.
- Amiro, B., A. Orchansky, and A. Sass, 2006: A perspective on carbon dioxide flux measurements using an open-path infrared gas analyzer in cold environments. *The 27th Conference on Agricultural and Forest Meteorology* P4. 7. May 22-25, 2006, San Diego, California, USA.
- Bakwin, P. S., K. J. Davis, C. Yi, S. C. Wofsy, J. W. Munger, L. Haszpra, and Z. Barcza, 2004: Regional carbon dioxide fluxes from mixing ratio data. *Tellus Series B-Chemical and Physical Meteorology*, **56**, 301-311.
- Bogoev, I., M. Helbig, and O. Sonnentag, 2014: On the importance of high-frequency air-temperature fluctuations for spectroscopic corrections of open-path carbon dioxide flux measurements. *EGU General Assembly Conference Abstracts*, **17**.
- Burba, G., 2013: Eddy covariance method for scientific, industrial, agricultural and regulatory applications: A field book on measuring ecosystem gas exchange and areal emission rates. *LI-Cor Biosciences*. Part 2.4, 78-79.
- Burba, G., D. Anderson, L. Xu, and D. McDermitt, 2005: Solving the off-season uptake problem: correcting fluxes measured with the LI-7500 for the effects of instrument surface heating. *Progress report of the ongoing study. PART II: RESULTS. Poster Presentation. AmeriFlux 2005 Annual Meeting, Boulder, Colorado*.
- Burba, G. G., D. K. McDermitt, A. Grelle, D. J. Anderson, and L. Xu, 2008: Addressing the influence of instrument surface heat exchange on the measurements of CO<sub>2</sub> flux from open - path gas analyzers. *Global Change Biology*, **14**, 1854-1876.
- Delpierre, N., D. Berveiller, E. Granda, and E. Dufrêne, 2015: Wood phenology, not carbon input, controls the interannual variability of wood growth in a temperate oak forest. *New Phytol.* **210**, 459-470

523 Detto, M., J. Verfaillie, F. Anderson, L. Xu, and D. Baldocchi, 2011: Comparing laser-based open- and  
 524 closed-path gas analyzers to measure methane fluxes using the eddy covariance method. *Agricultural and*  
 525 *Forest Meteorology*, **151**, 1312-1324.

526 Euskirchen, E., M. S. Bret-Harte, G. Scott, C. Edgar, and G. R. Shaver, 2012: Seasonal patterns of carbon  
 527 dioxide and water fluxes in three representative tundra ecosystems in northern Alaska. *Ecosphere*, **3**, 1-19.

528 Fratini, G., D. McDermitt, and D. Papale, 2014: Eddy-covariance flux errors due to biases in gas concentration  
 529 measurements: origins, quantification and correction. *Biogeosciences*, **11**, 1037-1051.

530 Grelle, A., and G. Burba, 2007: Fine-wire thermometer to correct CO<sub>2</sub> fluxes by open-path analyzers for  
 531 artificial density fluctuations. *Agricultural and Forest Meteorology*, **147**, 48-57.

532 Helbig, M., E. Humphreys, I. Bogoev, W. L. Quinton, K. Wischnweski, and O. Sonnentag, 2015: Effects of  
 533 biased CO<sub>2</sub> flux measurements by open-path sensors on the interpretation of CO<sub>2</sub> flux dynamics at  
 534 contrasting ecosystems. *EGU General Assembly Conference Abstracts*, **281**.

535 Helbig, M., and Coauthors, 2016: Addressing a systematic bias in carbon dioxide flux measurements with the  
 536 EC150 and the IRGASON open-path gas analyzers. *Agricultural and Forest Meteorology*, **228**, 349-359.

537 Hirata, R., T. Hirano, J. Mogami, Y. Fujinuma, K. Inukai, N. Saigusa, and S. Yamamoto, 2005: CO<sub>2</sub> flux  
 538 measured by an open-path system over a larch forest during the snow-covered season. *Phyton*, **45**, 347-351.

539 Horst, T. W., S. R. Semmer, and G. Maclean, 2015: Correction of a Non-orthogonal, Three-Component Sonic  
 540 Anemometer for Flow Distortion by Transducer Shadowing. *Boundary-Layer Meteorology*, **155**, 371-395.

541 Horst, T. W., R. Vogt, and S. P. Oncley, 2016: Measurements of Flow Distortion within the IRGASON  
 542 Integrated Sonic Anemometer and CO<sub>2</sub> /H<sub>2</sub>O Gas Analyzer. *Boundary-Layer Meteorology*, **160**, 1-15.

543 Jamieson, J. A., McFee, R. H., Plass, G. N., Grube, R. H. and Richards, R. G. 1963: Infrared Physics and  
 544 Engineering. McGraw-Hill, New York, 673.

Järvi, L., and Coauthors, 2009: Comparison of net CO<sub>2</sub> fluxes measured with open-and closed-path infrared gas analyzers in an urban complex environment. *Boreal Environment Research*, **14**, 499-514.

Kondo, F., K. Ono, M. Mano, A. Miyata, and O. Tsukamoto, 2014: Experimental evaluation of water vapour cross-sensitivity for accurate eddy covariance measurement of CO<sub>2</sub> flux using open-path CO<sub>2</sub> /H<sub>2</sub>O gas analysers. *Tellus B: Chemical and Physical Meteorology*, **66.1**, 23803.

Krishnan, P., T. A. Black, N. J. Grant, A. G. Barr, E. T. H. Hogg, R. S. Jassal, and K. Morgenstern, 2006: Impact of changing soil moisture distribution on net ecosystem productivity of a boreal aspen forest during and following drought. *Agricultural and Forest Meteorology*, **139**, 208-223.

Lafleur, P. M., and E. R. Humphreys, 2008: Spring warming and carbon dioxide exchange over low Arctic tundra in central Canada. *Global Change Biology*, **14**, 740-756.

Liu, R., Y. Li, and Q. X. Wang, 2012: Variations in water and CO<sub>2</sub> fluxes over a saline desert in western China. *Hydrological Processes*, **26**, 513-522.

Ma, J., R. Liu, L. S. Tang, Z. D. Lan, and Y. Li, 2014: A downward CO<sub>2</sub> flux seems to have nowhere to go. *Biogeosciences*, **11**, 6251-6262.

McDermitt, D., and Coauthors, 2011: A new low-power, open-path instrument for measuring methane flux by eddy covariance. *Appl. Phys. B*, **102**, 391-405.

Nakai, T., and K. Shimoyama, 2012: Ultrasonic anemometer angle of attack errors under turbulent conditions. *Agricultural and Forest Meteorology*, **162**, 14-26.

Nakai, T., M. K. van der Molen, J. H. C. Gash, and Y. Kodama, 2006: Correction of sonic anemometer angle of attack errors. *Agricultural and Forest Meteorology*, **136**, 19-30.

Ono, K., A. Miyata, and T. Yamada, 2008: Apparent downward CO<sub>2</sub> flux observed with open-path eddy covariance over a non-vegetated surface. *Theor Appl Climatol*, **92**, 195-208.

567 Peters, W., and Coauthors, 2007: An atmospheric perspective on North American carbon dioxide exchange:  
 568 CarbonTracker. *Proceedings of the National Academy of Sciences*, **104**, 18925-18930.

569 Schlesinger, W. H., 2017: An evaluation of abiotic carbon sinks in deserts. *Global Change Biology*, **23**, 25-27.

570 Serrano-Ortiz, P., A. S. Kowalski, F. Domingo, B. Ruiz, and L. Alados-Arboledas, 2008: Consequences of  
 571 Uncertainties in CO<sub>2</sub> Density for Estimating Net Ecosystem CO<sub>2</sub> Exchange by Open-path Eddy Covariance.  
 572 *Boundary-Layer Meteorology*, **126**, 209-218.

573 Wang, W., and Coauthors, 2016: Performance evaluation of an integrated open-path eddy covariance system in a  
 574 cold desert environment. *Journal of Atmospheric and Oceanic Technology*, 33(11), 2385-2399.

575 Webb, E. K., G. I. Pearman, and R. Leuning, 1980: Correction of flux measurements for density effects due to  
 576 heat and water vapour transfer. *Quarterly Journal of the Royal Meteorological Society*, **106**, 85-100.

577 Welles, JM, McDermitt, DK, 2005: Measuring carbon dioxide in the atmosphere. In: Hatfield, JL, Baker, JM  
 578 (Eds.), *Micrometeorology in Agricultural Systems*, 287-300

579 Welp, L. R., J. T. Randerson, and H. P. Liu, 2007: The sensitivity of carbon fluxes to spring warming and  
 580 summer drought depends on plant functional type in boreal forest ecosystems. *Agricultural and Forest*  
 581 *Meteorology*, **147**, 172-185.

582 Wohlfahrt, G., L. F. Fenstermaker, and J. A. Arnone, III, 2008: Large annual net ecosystem CO<sub>2</sub> uptake of a  
 583 Mojave Desert ecosystem. *Global Change Biology*, **14**, 1475-1487.

## Figure caption list

Figure 1. Locations of the 64 eddy flux sites used in this study.

Figure 2. Relationship between wintertime CO<sub>2</sub> flux ( $F_{c,a}$ ) and sensible heat ( $H$ ) at the Kubuqi shrub land site in China (site ID: CN-Kub\_s; panel a) and at the Brooks cropland site in the U. S. (site ID: US-Br3; panel b). Grey dots represent half-hourly data, and black dots and error bars represent bin-average values and standard deviations. Error bounds of the regression coefficients are  $\pm 1$  standard error.

Figure 3. Distribution of the slope parameter  $b$  ( $\mu\text{mol m}^{-2} \text{s}^{-1}$  per  $\text{W m}^{-2}$ ) according to vegetation type: ENF, Evergreen Needleleaf Forest; DBF, Deciduous Broadleaf Forests; GRA, Grasslands; WET, Permanent Wetlands; CRO, Croplands; OSH, Open Shrub lands; BAR, Barrens.

Figure 4. Comparison among three gas analyzer types of the slope parameter  $b$  ( $\mu\text{mol m}^{-2} \text{s}^{-1}$  per  $\text{W m}^{-2}$ ; gray bars) and the  $R^2$  value (white bars) of the linear regression between wintertime CO<sub>2</sub> flux and sensible heat flux. Error bars are  $\pm 1$  standard error.

Figure 5. Same as Figure 4 except for comparison among climate zones. The letters (a and b) mean statistical differences at  $p < 0.05$ .

Figure 6. The regression slope parameter  $b$  ( $\mu\text{mol m}^{-2} \text{s}^{-1}$  per  $\text{W m}^{-2}$ ) versus site mean air temperature (panel a) and absolute humidity (panel b). Different symbols represent different vegetation types.

Figure 7. The regression slope parameter  $b$  ( $\mu\text{mol m}^{-2} \text{s}^{-1}$  per  $\text{W m}^{-2}$ ) versus relative bias in the CO<sub>2</sub> concentration. Different symbols represent different analyzer types. The black line represents the theoretical relationship  $y = 0.05x$ .

Figure 8. Diurnal composite of the original uncorrected carbon flux (solid dots) and the corrected carbon flux (open dots) in December 2008 at the Kubuqi shrub land site (site ID: CN-Kub\_s).

Figure 9. Cumulated net ecosystem productivity at the Kubuqi shrub land site (site ID: CN-Kub\_s). A positive NEP indicates that the ecosystem is a sink for atmospheric CO<sub>2</sub>, and vice versa.

Figure 10. Cumulated net ecosystem productivity at the grass land site in Austria (site ID: AT-Neu). A positive NEP indicates that the ecosystem is a sink for atmospheric CO<sub>2</sub>, and vice versa.

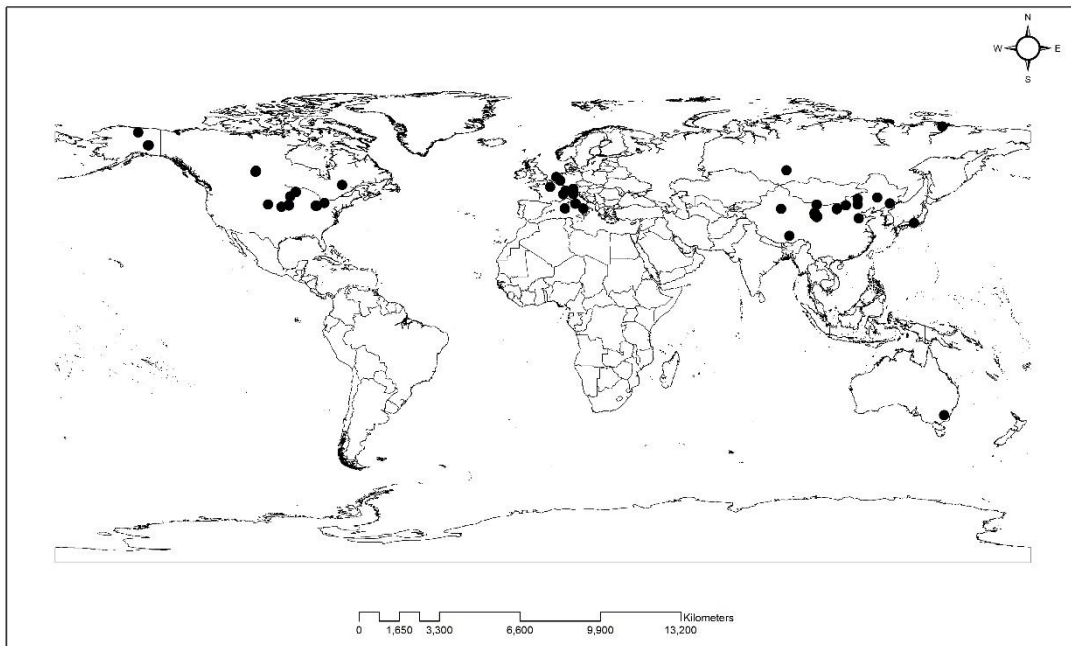


Figure 1. Locations of the 64 eddy flux sites used in this study.



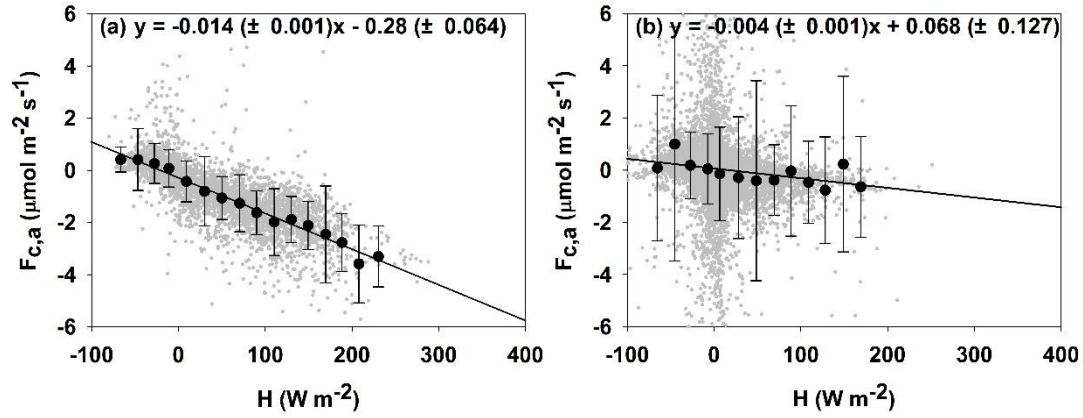


Figure 2. Relationship between wintertime CO<sub>2</sub> flux ( $F_{c,a}$ ) and sensible heat ( $H$ ) at the Kubuqi shrub land site in China (site ID: CN-Kub\_s; panel a) and at the Brooks cropland site in the U. S. (site ID: US-Br3; panel b). Grey dots represent half-hourly data, and black dots and error bars represent bin-average values and standard deviations. Error bounds of the regression coefficients are  $\pm 1$  standard error.

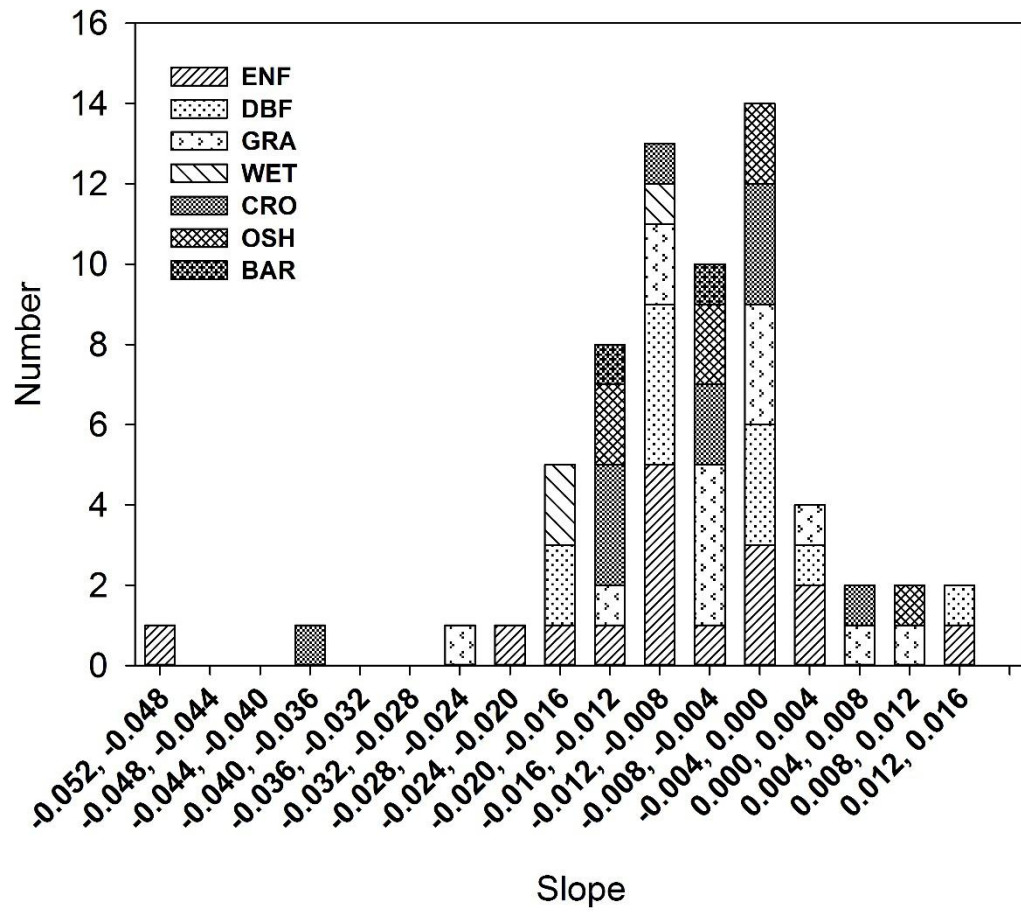


Figure 3. Distribution of the slope parameter  $b$  ( $\mu\text{mol m}^{-2} \text{s}^{-1} \text{ per W m}^{-2}$ ) according to vegetation type: ENF, Evergreen Needleleaf Forest; DBF, Deciduous Broadleaf Forests; GRA, Grasslands; WET, Permanent Wetlands; CRO, Croplands; OSH, Open Shrub lands; BAR, Barrens.

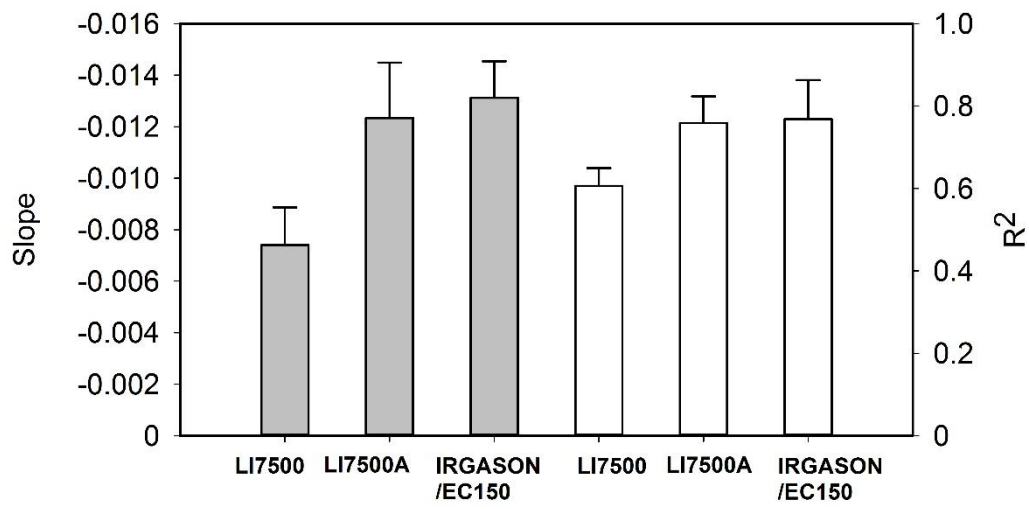


Figure 4. Comparison among three gas analyzer types of the slope parameter  $b$  ( $\mu\text{mol m}^{-2} \text{s}^{-1}$  per  $\text{W m}^{-2}$ ; gray bars) and the  $R^2$  value (white bars) of the linear regression between wintertime  $\text{CO}_2$  flux and sensible heat flux. Error bars are  $\pm 1$  standard error.

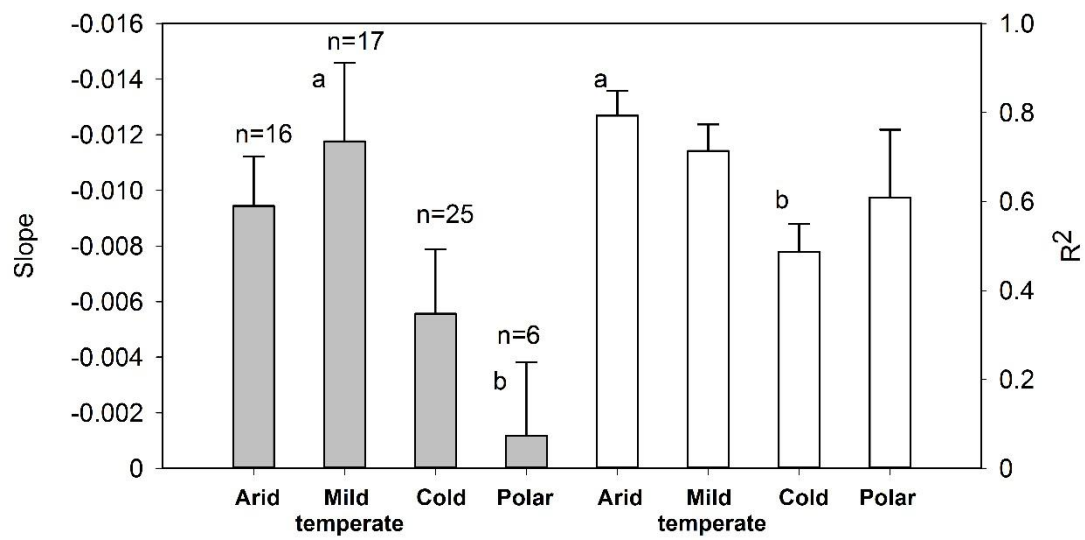


Figure 5. Same as Figure 4 except for comparison among climate zones. The letters (a and b) mean statistical differences ( $p < 0.05$ ).

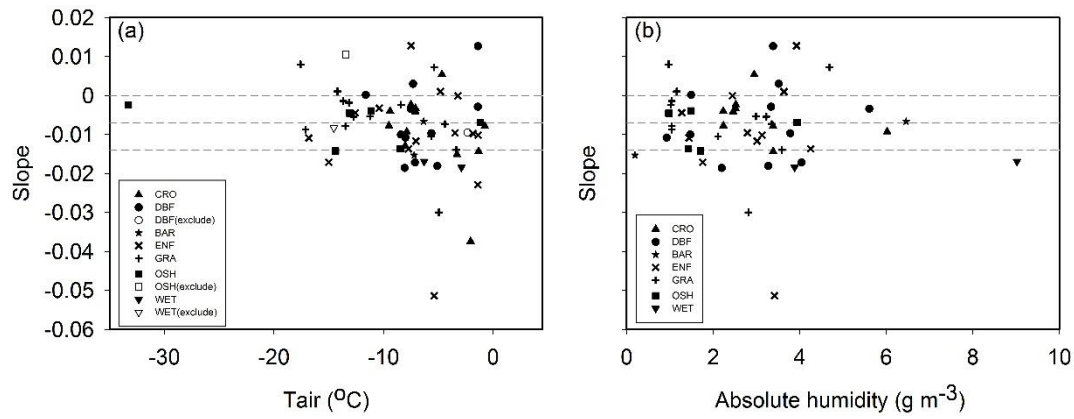


Figure 6. The regression slope parameter  $b$  ( $\mu\text{mol m}^{-2} \text{s}^{-1}$  per  $\text{W m}^{-2}$ ) versus site mean air temperature (panel a) and absolute humidity (panel b). Different symbols represent different vegetation types. The temperature and humidity are mean values from the half-hourly or hourly observations selected for the slope analysis.

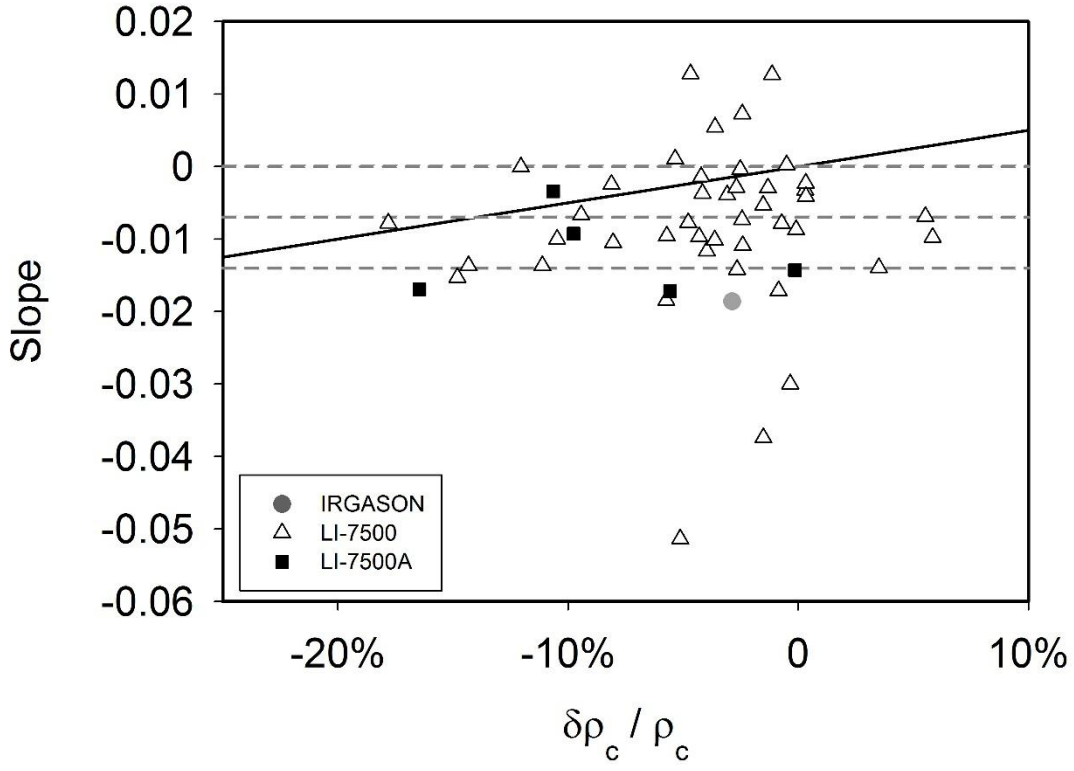


Figure 7. The regression slope parameter  $b$  ( $\mu\text{mol m}^{-2} \text{s}^{-1}$  per  $\text{W m}^{-2}$ ) versus relative bias in the  $\text{CO}_2$  concentration. Different symbols represent different analyzer types. The black line represents the theoretical relationship  $y = 0.05x$ .

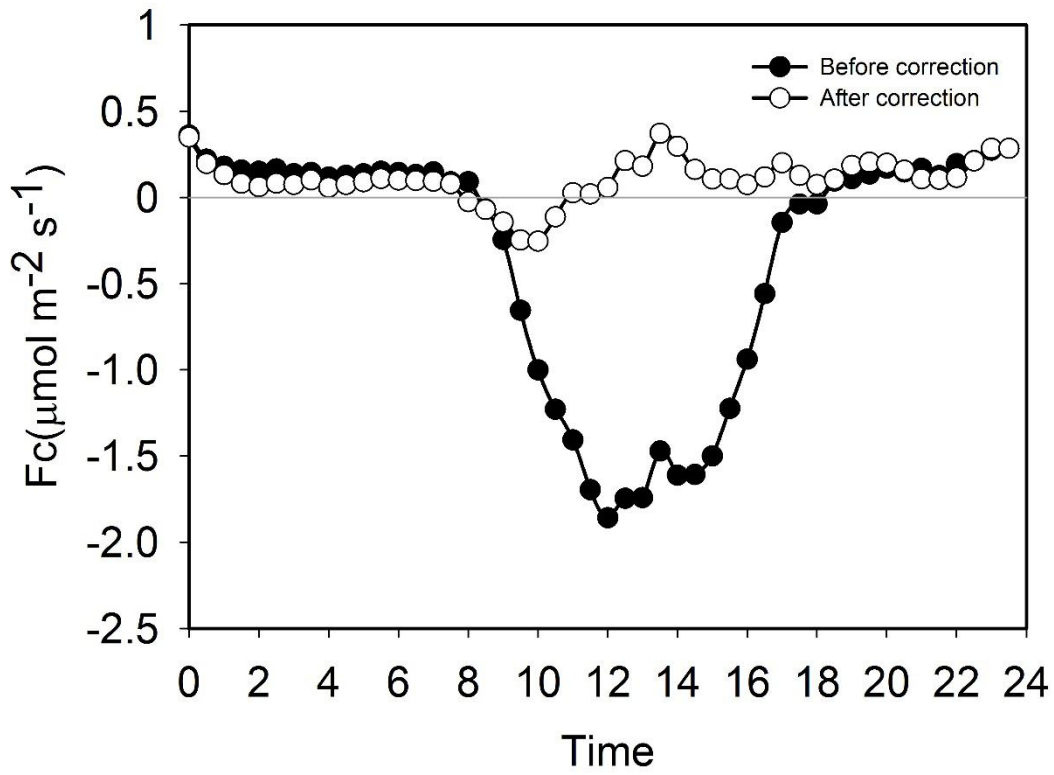


Figure 8. Diurnal composite of the original uncorrected carbon flux (solid dots) and the corrected carbon flux (open dots) in December 2008 at the Kubeqi shrub land site (site ID: CN-Kub\_s).

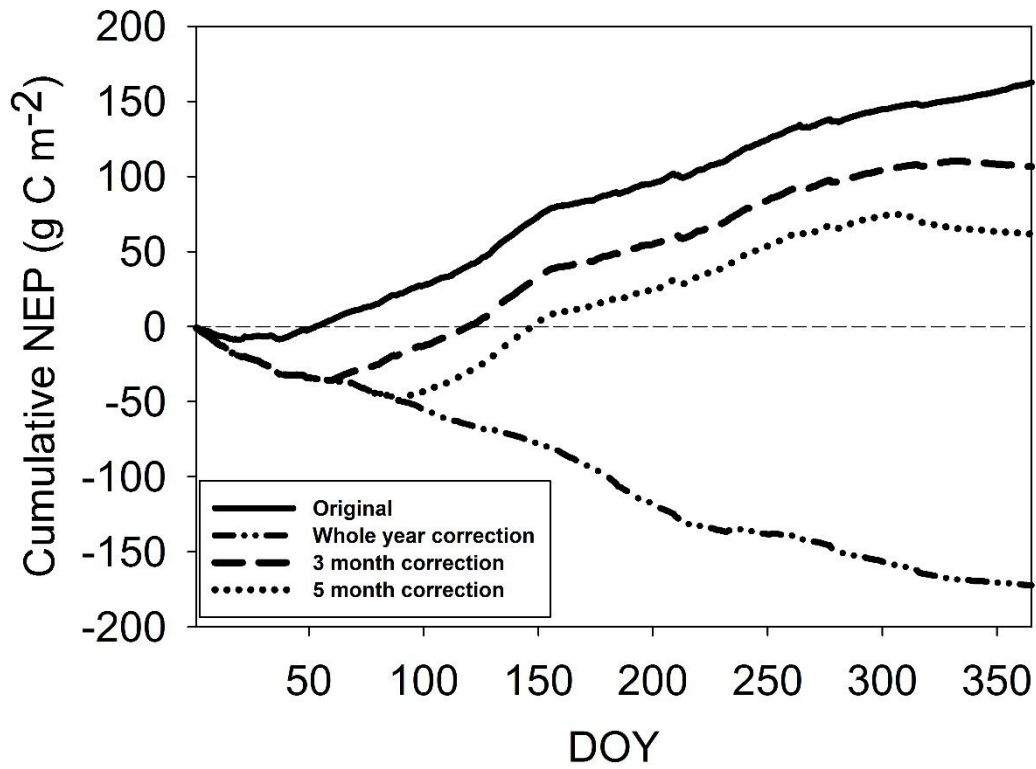


Figure 9. Cumulated net ecosystem productivity at the Kubuqi shrub land site (site ID: CN-Kub\_s). A positive NEP indicates that the ecosystem is a sink for atmospheric CO<sub>2</sub>, and vice versa.



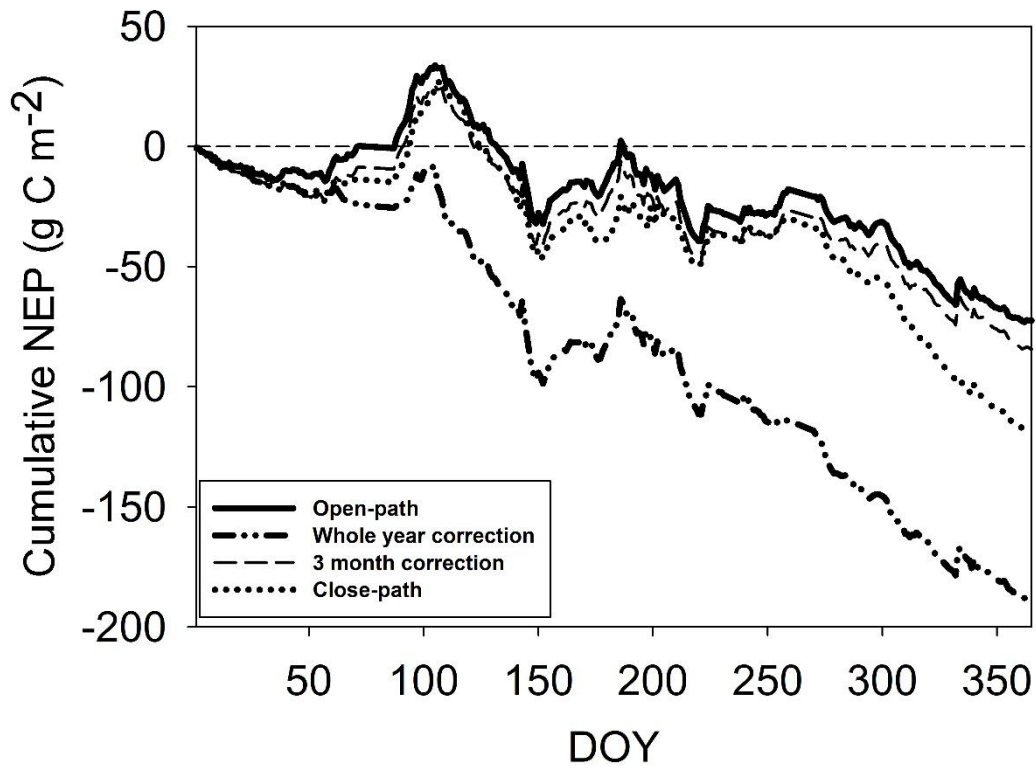


Figure 10. Cumulated net ecosystem productivity at the grass land site in Austria (site ID: AT-Neu). A positive NEP indicates that the ecosystem is a sink for atmospheric CO<sub>2</sub>, and vice versa.